

# Thin Molecularly Imprinted Polymer Films via Reversible Addition–Fragmentation Chain Transfer Polymerization

Maria-Magdalena Titirici and Börje Sellergren\*

INFU, Universität Dortmund, Otto-Hahn-Strasse 6, 44122 Dortmund, Germany

Received September 26, 2005. Revised Manuscript Received December 16, 2005

Mesoporous silica beads modified with an azo initiator were used for grafting of cross-linked molecularly imprinted polymers through reversible addition–fragmentation chain transfer (RAFT) mediated polymerization. The RAFT mediation allowed an efficient control of the grafting process and led to suppression of the solution propagation preventing any visible gel formation. Thus, graft copolymerization of methacrylic acid and ethylene glycol dimethacrylate using 2-phenylprop-2-yl-dithiobenzoate as the chain transfer agent and in the presence of L-phenylalanine anilide as the template led to imprinted thin film composite beads. The resulting composites were characterized by Fourier transform infrared spectroscopy, nitrogen sorption analysis, elemental analysis, fluorescence microscopy, and scanning electron microscopy and as stationary phases in chromatography. This indicated the presence of thin homogeneous films (thickness: 1–2 nm) containing imprinted sites for the template (L-phenylalanine anilide). The resulting materials proved to be highly selective chiral stationary phases resulting in baseline separations of the template racemate and of structurally analogous racemates within a few minutes. These results were comparable with results obtained for materials prepared in the absence of RAFT mediation with the notable difference being the absence of detectable solution gelation using RAFT.

## Introduction

Molecular imprinting is an attractive concept for the generation of polymer-based molecular recognition elements tailor-made for a given target or group of target molecules.<sup>1–4</sup> This is shown by the intense research efforts aimed at developing such molecularly imprinted polymers (MIPs) toward a wide range of applications including solid-phase extraction, chemical sensing, drug delivery, catalysis, and chiral separations to name a few. Traditional techniques used to prepare MIPs most often result in materials exhibiting high affinity and selectivity but low capacity and poor site accessibility for the target molecule.<sup>5</sup> These MIPs consist of particles of irregular shape obtained through a low yielding crushing sieving process. Previous attempts to address these problems have involved the use of well-established bead polymerization techniques either in two-phase systems by suspension polymerization<sup>6,7</sup> or from one-phase systems by precipitation polymerization.<sup>8</sup> Although typically high yielding processes, these techniques often involve a complicated

factor optimization when new templates are introduced and have not led to significant improvements in the molecular recognition or kinetic properties of the materials. Therefore, MIP synthesis techniques decoupling the imprinting step from the generation of a particular polymer morphology would be attractive. This can be achieved by the use of grafting techniques where one distinguishes between “grafting to” and “grafting from” techniques, the latter referring to polymerizations initiated from a preformed polymer or the surface of a solid support.<sup>9</sup> Recently, the “grafting from” technique has been used by several research groups to produce imprinted polymer layers on various substrates.<sup>10–14</sup>

Our group reported on “grafting from” techniques for the synthesis of MIP composite materials with improved kinetic properties.<sup>11–13</sup> The first of these consisted of the use of immobilized azo initiators which allowed the synthesis of

\* To whom correspondence should be addressed. E-mail: borje@infu.uni-dortmund.de.

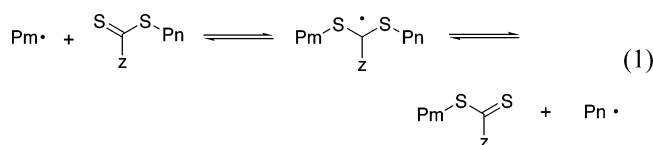
- (1) Sellergren, B., Ed. *Molecularly Imprinted Polymers: Man made mimics of antibodies and their applications in analytical chemistry*; Techniques and instrumentation in analytical chemistry; Elsevier Science B.V.: Amsterdam, 2001; Vol. 23.
- (2) Hall, A. J.; Emgenbroich, M.; Sellergren, B. In *Templates in Chemistry II*; Schalley, C. A., Vögtle, F., Dötz, K. H., Eds.; Topics in Current Chemistry; Springer-Verlag: Heidelberg, 2005; Vol. 249, pp 317–349.
- (3) Yan, M., Ramström, O., Eds. *Molecularly Imprinted Materials: Science and Technology*; Marcel Dekker: New York, 2005.
- (4) Piletsky, S. A., Nicholls, I. A., Turner, A. P. F., Eds. *Molecularly imprinted polymers*; Landes Biosciences: 2004 (<http://www.eurekah.com>).
- (5) Chen, Y.; Kele, M.; Sajonz, P.; Sellergren, B.; Guiochon, G. *Anal. Chem.* **1999**, *71*, 928–938.

- (6) Mayes, A. G. In *Molecularly Imprinted Polymers: Man made mimics of antibodies and their applications in analytical chemistry*; Sellergren, B., Ed.; Techniques and instrumentation in analytical chemistry; Elsevier Science B.V.: Amsterdam, 2001; Vol. 23, pp 305–324.
- (7) Kempe, H.; Kempe, M. *Macromol. Rapid Commun.* **2004**, *25*, 315–320.
- (8) Wang, J.; Cormack, P. A. G.; Sherrington, D. C.; Khoshdel, E. *Angew. Chem., Int. Ed.* **2003**, *42*, 5336–5338.
- (9) Prucker, O.; Rühle, J. *Macromolecules* **1998**, *31*, 602–613.
- (10) Piletsky, S. A.; Matuschewski, H.; Schedler, U.; Wilpert, A.; Piletska, E. V.; Thiele, T. A.; Ulbricht, M. *Macromolecules* **2000**, *33*, 3092–3098.
- (11) Sulitzky, C.; Rückert, B.; Hall, A. J.; Lanza, F.; Unger, K.; Sellergren, B. *Macromolecules* **2002**, *35*, 79–91.
- (12) Rückert, B.; Hall, A. J.; Sellergren, B. *J. Mater. Chem.* **2002**, *12*, 2275–2280.
- (13) Sellergren, B.; Rückert, B.; Hall, A. J. *Adv. Mater.* **2002**, *14* (17), 1204–1208.
- (14) Wei, X.; Li, X.; Husson, S. M. *Biomacromolecules* **2005**, *6*, 1113–1121.

thin film MIP composites with much improved mass transfer characteristics.<sup>11</sup> However, as a result of only one point attachment of the initiators, solution polymerization and resulting phase separation could not be completely avoided. This limits the usefulness of the method.

This problem was overcome by the use of immobilized dithiocarbamate initiators (commonly referred to as iniferters) where the mobile radical formed upon decomposition is stable and poor at propagating chains.<sup>12,13</sup> However, as will be shown in forthcoming publications,<sup>15</sup> the iniferter grafted composites are inferior to the azo-grafted counterparts when assessed in the chromatographic mode.

To address this problem we have here investigated means to control the azoinitiated grafting through the addition of chain transfer agents. The use of dithioesters has proven particularly versatile in this regard.<sup>16–19</sup> These can be structurally tuned to allow polymerization through the so-called RAFT (reversible addition–fragmentation chain transfer) mechanism. This features a fast capping of the majority of the propagating chains by the RAFT agent followed by the establishment of a dynamic equilibrium between growing and dormant chains according to eq 1:



where Pm and Pn are propagating chains and z is an electron-withdrawing substituent.

This results in a low radical concentration near the surface, hence, less termination by radical recombination, slower kinetics, and linear time-conversion curves. Furthermore, interchain equilibration reduces chain length dispersity and heterogeneity of the grafts. The focus of this work is the synthesis of MIP composites using the “grafting from” method by controlled radical polymerization (CRP) via RAFT. The materials can be prepared in a short time and exhibit superior mass transfer properties compared to the traditional imprinted solution polymerized networks.

### Experimental Section

**Materials.** BOC-L-phenylalanine, *N,N'*-dicyclohexylcarbodiimide (DCC), trifluoroacetic acid, ethylene glycol dimethacrylate (EDMA), methacrylic acid (MAA), (3-aminopropyl)triethoxysilane (APS), and ethyl chloroformate were obtained from Aldrich (Deisenhofen, Germany). EDMA was purified by washing consecutively with 10% aqueous NaOH, water, brine, and finally water. After drying over MgSO<sub>4</sub>, pure, dry EDMA was obtained by distillation under a reduced pressure. MAA was purified by distillation under a reduced pressure. 1-Hydroxybenzotriazole hydrate (HOBt), 4,4'-azobis(4-cyanopentanoic acid) (ACPA), 3-amino-quinoline, ethyl acetate, methanol, and acetic acid (AcOH) were obtained from Fluka

**Table 1. Characterization of the Modified Silica Supports Used for Grafting**

modified support <sup>a</sup>	%C	%N	area density <sup>b</sup> ( $\mu\text{mol}/\text{m}^2$ )	coverage <sup>c</sup> (%)	distance <sup>d</sup> (nm)
Si-APS	3.79	1.34	2.9	36	0.8
Si-APS-ACPAa	5.98	1.98	0.33	4.1	2.2
Si-APS-ACPAb	11.76	3.93	1.5	18	1.1

<sup>a</sup> The immobilizations were performed in two steps by consecutive coupling of APS and ACPA on Si-100 silica beads, and the modified supports were analyzed by elemental analysis of carbon and nitrogen. The Si-100 silica beads (10  $\mu\text{m}$  average particle size) were mesoporous as judged from the nitrogen sorption data ( $S = 360 \text{ m}^2/\text{g}$ ;  $d_p = 13 \text{ nm}$ ,  $V_p = 1.39 \text{ mL/g}$ ). <sup>b</sup> The area density ( $D$ ) was calculated from the increase in nitrogen content after the corresponding coupling as  $D = m_N/(M_N S)$ , where  $m_N = N\%/(100 - N\%M_w/M_N)$ ,  $M_w$  = molecular weight of immobilized silane (step 1) or azo initiator (step 2),  $M_N$  = weight of nitrogen per mole of immobilized species, and  $S$  = surface area of the silica support.  $M_w$  and  $M_N$  were calculated assuming complete conversion of the silane. <sup>c</sup> The coverage ( $C$ ) was calculated as  $C = 100 \times D/8$ , assuming a maximum silanol group density of  $8 \mu\text{mol}/\text{m}^2$ . <sup>d</sup> The average distance  $d_L$  (nm) between the coupled ligands assuming a random ligand distribution was calculated as  $d_L = [10^{18}/(D \times 10^{-16} \times N)]^{1/2}$ , where  $N$  is Avogadro's number.

(Deisenhofen, Germany). Benzoic acid, 2-phenyl-2-propanol, and phosphorus pentasulfide were obtained from Acros Organics (Geel, Belgium). Concentrated hydrochloric acid, dichloromethane (DCM), benzene, and acetonitrile (MeCN) were obtained from Merck (Darmstadt, Germany). BOC-D-phenylalanine and L- and D-phenylalanine *p*-nitroanilide were purchased from Bachem (Heidelberg, Germany). The templates L- and D-phenylalanine anilide (L-PA, D-PA) were synthesized following a previously described procedure.<sup>11</sup> Aniline was obtained from Aldrich.

Anhydrous solvents, dimethyl formamide, toluene, and tetrahydrofuran were purchased from Fluka and used as received. The silica research samples Si-100 were supplied by Dr. D. Lubda from Merck (Darmstadt).

These were modified with azo initiator in two steps as previously reported.<sup>11</sup> Silanization of rehydroxylated silica with APS was followed by condensation of the initiator ACPA with the surface amino groups to give the initiator modified supports listed in Table 1.

The RAFT agent, 2-phenylprop-2-yl-dithiobenzoate, was synthesized according to the method reported by Benicewicz et al. by refluxing benzoic acid and 2-phenyl-2-propanol in the presence of phosphorus pentasulfide in benzene.<sup>20</sup>

**Apparatus.** The HPLC measurements were carried out on Hewlett-Packard HP 1050 instruments (Agilent Technologies, Waldbronn, Germany). The fluorescently labeled silica particles were investigated using a LEICA DM R fluorescence microscope (Benzheim, Germany). The grafting yields were estimated from elemental microanalysis obtained using a “CHN-rapid” HERAEUS analyzer (Hanau, Germany). Fourier transform infrared (FT-IR) spectroscopy was performed using a NEXUS FT-IR spectrometer (Thermo Electron Corporation, Dreieich, Germany).

The particle morphology was determined using a scanning electron microscope SEM Hitachi S 4500.

Nitrogen sorption measurements were performed on a Quantachrome Autosorb 6B (Quantachrome Corporation, Boynton Beach, FL) automatic adsorption instrument. Prior to measurements, 100–150 mg of the samples was heated at 60 °C under high vacuum ( $10^{-5} \text{ Pa}$ ) for at least 12 h. The specific surface areas ( $S$ ) were evaluated using the BET method, the specific pore volumes ( $V_p$ ) were evaluated following the Gurvitch method, and the average pore diameter ( $d_p$ ) was evaluated using the BJH theory.

(15) Titirici et al. Manuscript in preparation.

(16) Chiefari, J.; Chong, Y. K.; Ercole, F.; Kristina, J.; Jeffrey, J.; Le, P. T.; Mayadunne, R. T. A.; Meijs, G. F.; Moad, C. L.; Moad, G.; Rizzardo, E.; Thang, S. H. *Macromolecules* **1998**, *31*, 5559.

(17) Goto, A.; Sato, K.; Tsujii, Y.; Fukuda, T.; Moad, G.; Rizzardo, E.; Thang, S. H. *Macromolecules* **2001**, *34*, 402–408.

(18) Baum, M.; Brittain, W. J. *Macromolecules* **2002**, *35*, 610–615.

(19) Tsuji, Y.; Ejaz, M.; Sato, K.; Goto, A.; Fukuda, T. *Macromolecules* **2001**, *34*, 8872–8878.

(20) Sudalai, A.; Kanagasabapathy, S.; Benicewicz, B. C. *Org. Lett.* **2000**, *2*, 3213–3216.

**Grafting of Polymer on Silica.** The grafting was performed in specially designed tubes containing 1 g of azo-initiator modified silica particles suspended in a polymerization mixture containing L-PA (0.240 g, 1 mmol), RAFT agent (0.20 g, 0.74 mmol), MAA (0.68 mL, 8 mmol), and EDMA (7.6 mL, 40 mmol) dissolved in 11 mL of dry toluene. After sealing, mixing, and purging the mixture with nitrogen, polymerization was initiated by UV irradiation, using a high-pressure mercury vapor lamp at 15 °C, and allowed to continue for 60, 90, 120, or 240 min, respectively, with continuous nitrogen purging. After polymerization, the samples were extracted with methanol using a Soxhlet apparatus for 24 h. Non-imprinted control polymer composites were prepared as described above but without addition of the template. A parallel series of composites were prepared in the absence of RAFT agent.

**HPLC Measurements and Evaluation.** The composite materials were slurry packed into stainless steel columns (120 × 4.5 mm), using MeOH/H<sub>2</sub>O (80:20, v/v) as the pushing solvent, and evaluated chromatographically using as the mobile phase MeCN/sodium acetate buffer, 0.01 M, pH 4.8 (70:30, v/v). The flow rate was 1 mL/min, and 10 μL aliquots of 1 mM solutions of pure enantiomers or racemate were injected. The elution was monitored at 242 nm. The retention factors ( $k_L$  and  $k_D$ ) and the separation factor ( $\alpha$ ) were calculated using the following formulas:  $k_L = (t_L - t_0)/t_0$ ,  $k_D = (t_D - t_0)/t_0$ , and  $\alpha = k_L/k_D$ , where  $t_L$  is the retention time of the L-enantiomer,  $t_D$  is the retention time of the D-enantiomer, and  $t_0$  is the retention time of the void marker, acetone.

**Coupling of the Fluorescence Label.** The polymer modified silica (0.04 g), HOBt (1.1 equiv), and DCC (2 equiv) were mixed in dry DCM (20 mL) and stirred for 30 min before a solution of 3-aminoquinoline (1.1 equiv based on the theoretical amount of COOH groups in polymer) in DCM was added dropwise. The suspension was stirred for 12 h and filtered. The remaining solid was washed consecutively with DCM and ethyl acetate.

**Film Thickness Calculations.** The calculation of the film thickness  $d$  (nm) was performed assuming a homogeneous grafted layer as follows.

from elemental analysis

$$d = \frac{m_c M_w}{M_c \rho S} \times 10^3 \quad (2)$$

$$m_c = \frac{\%C}{100 - \left( \frac{\%CM_w}{M_c} \right)} \quad (3)$$

where  $m_c$  = weight of carbon of the grafted polymer per gram of bare silica support,  $M_w$  = weighted average molecular weight of the grafted polymer assuming stoichiometric incorporation of reactive monomers,  $M_c$  = weighted average molecular weight of the carbon fraction of the grafted polymer,  $\rho$  = weighted average density of monomers (g mL<sup>-1</sup>), and  $S$  = specific surface area of the bare silica support (m<sup>2</sup> g<sup>-1</sup>).

from average pore size

$$d = \frac{d_{pi} - d_{pf}}{2} \quad (4)$$

where  $d_{pi}$  = pore diameter of the original starting material and  $d_{pf}$  = pore diameter of the final composite.

gravimetrically

$$d = \frac{\Delta m}{\rho S} \times 10^3 \quad (5)$$

where  $\Delta m$  = weight increase after grafting.

**Table 2. Characterization of MIP Composites Prepared by Grafting from Silica in the Presence or Absence of RAFT Agent**

composite <sup>a</sup>	polym. time (min)	%C	%S	$\Delta m$ (g/g)	$S^b$ (m <sup>2</sup> /g)	$d_p^b$ (nm)	$V_p^b$ (mL/g)
C <sub>R</sub> <sup>60</sup>	60	15.6	0.32	0.35	192	11.5	0.66
C <sub>R</sub> <sup>90</sup>	90	17.4	0.31	0.42	192	11.5	0.69
C <sub>R</sub> <sup>120</sup>	120	18.7	0.29	0.51	193	11.4	0.65
C <sub>R</sub> <sup>240</sup>	240	19.9	0.30	0.58	181	9.9	0.59
C <sup>60</sup>	60	16		0.39	285	10.6	0.70
C <sup>90</sup>	90	21		0.52	280	10.2	0.63
C <sup>120</sup>	120	23		0.97	265	9.0	0.60

<sup>a</sup> The composites were prepared by grafting of imprinted polymers in the presence (C<sub>R</sub>) or absence (C) of RAFT agent for the times indicated using the supports Si-APS-ACPAb and Si-APS-ACPAA, respectively (see Table 1). <sup>b</sup> BET specific surface area ( $S$ ), specific pore volume ( $V_p$ ), and average pore diameter ( $d_p$ ) were calculated from nitrogen adsorption measurements.

## Results and Discussion

Grafting of polymers from surfaces of solid supports via an initiation step localized at the surface has been shown to result in densely grafted polymer films with tunable thickness.<sup>9</sup> The specific surface area of the support material determines the average thickness of the grafted polymer films at a given grafting density. Thus, composites with identical elemental composition may exhibit thin or thick films depending on whether high or low surface area supports are used.<sup>11</sup> We previously showed that L-PA imprinted composites prepared from high surface area silica with an average pore size of 10 nm (Si-100) exhibited enhanced chromatographic efficiency and enantioselectivity compared to a corresponding low surface area composite.<sup>11</sup> These composites featured thin films with average apparent thickness of only 1 nm below which no imprinted memory was observed. With this as a bench mark we synthesized ACPA modified Si-100 by consecutive coupling of APS to rehydroxylated silica followed by coupling of ACPA. The initiator density was hereby tuned to be low (0.33 μmol/m<sup>2</sup>) or high (1.5 μmol/m<sup>2</sup>) allowing kinetic effects and the influence of the distance between polymer anchoring points (see Table 1) on the imprinting efficiency to be investigated.

The ACPA modified supports were subsequently used for the grafting of imprinted polymer films (see Figure 1) according to our previously described procedure<sup>11</sup> but in the presence or absence of the RAFT agent, 2-phenylprop-2-yl-dithiobenzoate.

Thus, 1 g of silica was suspended in 20 mL of prepolymerization solution consisting of template (L-PA), functional monomer (MAA), and cross-linking monomer (EDMA) in toluene. The grafting was thereafter performed by UV initiated low-temperature polymerizations for defined periods of time under continuous nitrogen purging. After Soxhlet extraction of the particles they were characterized by gravimetry, IR spectroscopy, nitrogen sorption analysis, elemental analysis (Table 2), scanning electron microscopy, and fluorescence microscopy.

As expected, the kinetics of the grafting was faster in absence than in the presence of RAFT agent. This appeared clearly from a comparison of the grafting in the presence of the high and low initiator supports. In absence of control, only the low initiator support (Si-APS-ACPAA) produced

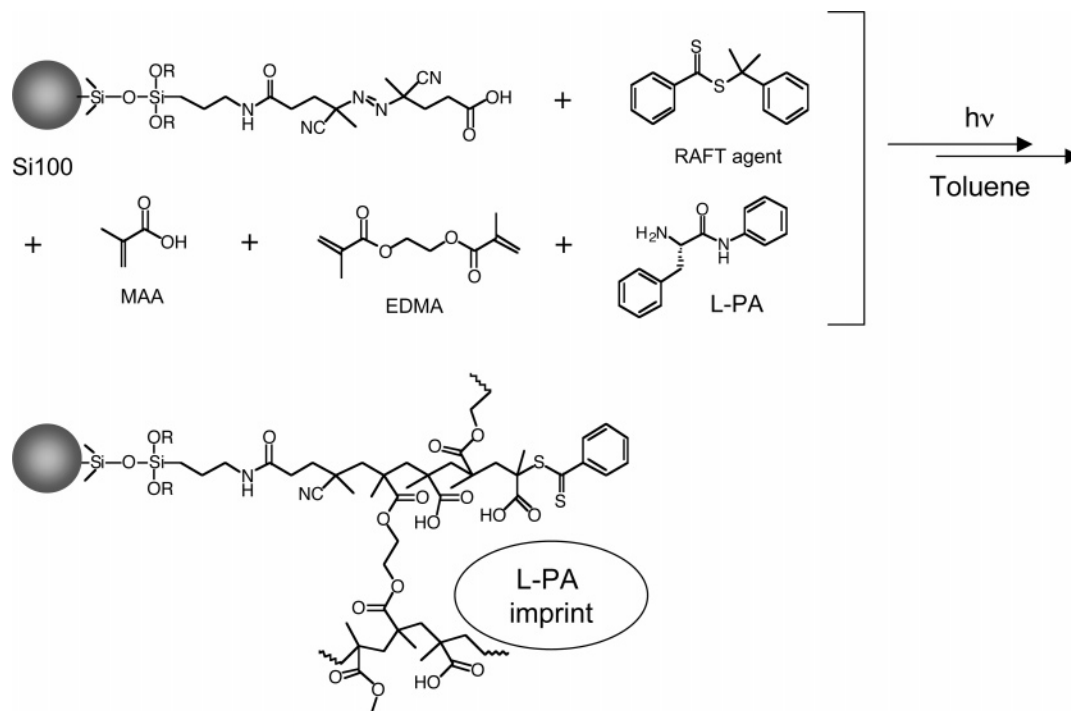


**Figure 1.** Scheme depicting the grafting of L-phenylalanine anilide (L-PA) imprinted polymer films from porous silica supports controlled by addition of RAFT agent.

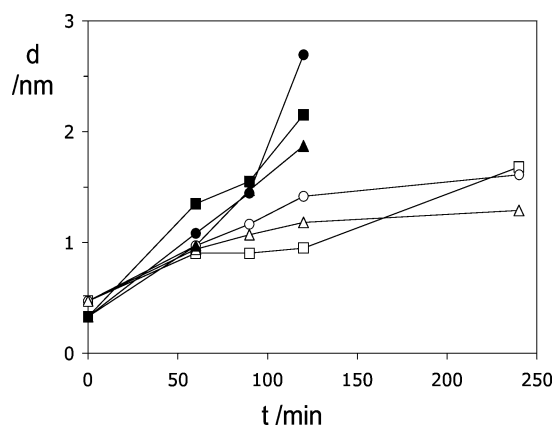


**Figure 2.** Average thickness ( $d$ ) of the grafted polymer films versus time of polymerization. The thickness was estimated on the basis of the average pore diameter (squares), gravimetrically (circles), and the carbon content (triangles) as described in Experimental Section. Filled and open symbols represent grafting in the absence and presence of RAFT agent, respectively. The thickness at the start was estimated from the carbon content of Si-APS-ACPAA (filled symbols) and Si-APS-ACPAB (open symbols), respectively.

grafted films with no detrimental macrogelation whereas premature gelation was observed using the high initiator support (Si-APS-ACPAB). This contrasted with grafting in the presence of the RAFT agent where the use of the high initiator support (Figure 2) was possible without any visible gelation. In agreement with this result, no polymer-related signals were observed in the  $^1\text{H}$  NMR spectrum taken of the remaining monomer solution after grafting in the presence of RAFT agent.

The effect of the RAFT agent is well-illustrated in Figure 3 showing the different textures of the obtained particles. Whereas the particles prepared via the RAFT mediated grafting appear smooth (Figure 3A) with no agglomeration (Figure 3B) and no visible nongrafted polymer, absence of

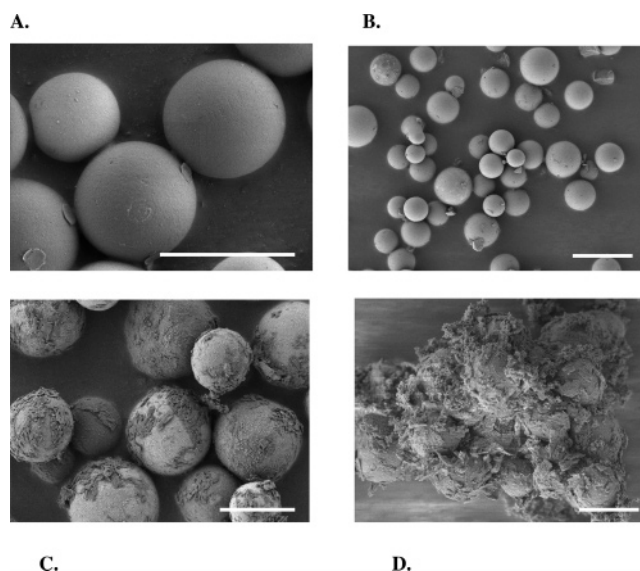


**Figure 3.** Scanning electron micrographs of the imprinted composite materials after a reaction time of 120 min (A, C, D) or 240 min (B). (A, B) Composites prepared using Si-APS-ACPAB ( $D = 1.5 \mu\text{mol}/\text{m}^2$ ) as initiator modified support in the presence of RAFT agent. (C, D) Composites prepared using (C) Si-APS-ACPAA ( $D = 0.33 \mu\text{mol}/\text{m}^2$ ) or (D) Si-APS-ACPAB ( $D = 1.5 \mu\text{mol}/\text{m}^2$ ) in the absence of RAFT agent. The bar represents a distance of 10  $\mu\text{m}$  (A, C, D) or 20  $\mu\text{m}$  (B).

control led to composites with extensive solution polymerization (Figure 3C) leading to complete immobilization of the silica particles at higher conversions (Figure 3D).

The presence of homogeneously grafted films was confirmed by comparing the film thickness estimated by three independent methods (Figure 2). The calculations based on elemental and gravimetric analysis assumed a stoichiometric incorporation of the monomers and a density of the grafts identical to the liquid monomers whereas the calculation based on the average pore size was performed with reference to the average pore size of the native silica (Table 2).

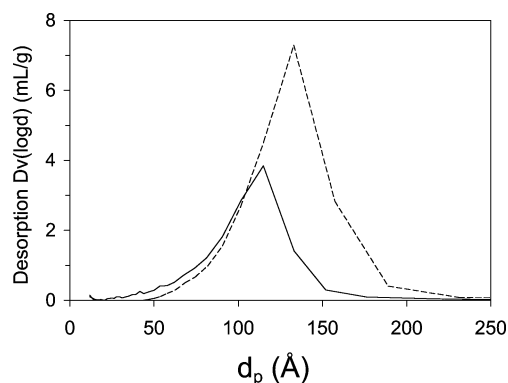


**Figure 4.** Pore size distribution of the bare silica support (dashed line) and  $C_R^{90}$  (solid line) calculated from the desorption branch of the isotherm obtained from nitrogen sorption measurements.

As can be seen in Figure 2, the three methods gave similar thicknesses providing strong evidence for the presence of homogeneously grafted films. It is also obvious from the similar widths of the pore size distribution of the materials measured before and after grafting (Figure 4) that the majority of pores measured stems from those of the silica support.

Additional evidence for the homogeneity of the grafted polymer films was obtained by fluorescence microscopy of particles labeled with the fluorescent dye 3-aminoquinoline (Figure 5). For a given grafting density the composites prepared in the presence of RAFT agent exhibited a more intense fluorescence and less interparticle intensity variations compared to composites prepared in absence of RAFT. This indicates a higher coupling yield in the former case presumably due to more accessible functional groups.

In addition to the imprinted composites, corresponding non-imprinted control composites were prepared. As seen in Figure 6 the imprinted and non-imprinted composites gave nearly identical carbon contents indicating a minimal influence of the template on the polymerization kinetics under the present conditions.

The particles were thereafter slurry packed into HPLC columns ( $120 \times 4.5$  mm) and evaluated using an aqueous mobile phase (MeCN/sodium acetate buffer, 0.01 M, pH 4.8, 70:30, v/v) for their ability to resolve and retain the racemate corresponding to the template (D,L-PA). The column efficiencies determined from the void marker (acetone) were acceptable (ca. 10 000 plates/m) indicating that the columns

had been properly packed. The elution profiles resulting from the kinetics investigation are seen in Figure 7. First of all, the non-imprinted control composites did not display any enantioselectivity and retained the racemate weakly close to the void fraction.

Concerning the imprinted composites, as we reported previously, the average thickness of the imprinted films has to exceed 1 nm to show any sign of memory for the template.<sup>11</sup> This was confirmed also for the RAFT mediated grafting. Thus, the composite prepared using the shortest polymerization time (60 min) exhibited only partial resolution and weak retention of the racemate. Longer grafting times resulted in a dramatic increase in resolution and retention of the racemate. In this context, it is noted that, while the retention of the racemate increased significantly, the enantioselectivity did not follow this trend within this thickness interval. This suggests that increased grafting time leads to an increase in the number of sites, rather than enhancing their selectivity per se.

The composites furthermore exhibited a unique dependence of enantioselectivity and resolution on the sample load. As seen in Figure 7, lowering the sample load from 10 to 5 nmol resulted in a higher separation factor and an increased peak width of the enantiomer corresponding to the template. This indicates the presence of a heterogeneous distribution of sites with slowly exchanging high energy sites which become saturated within this concentration interval.<sup>5</sup>

This is further corroborated by the elution profile obtained upon injection of the racemate of the template analogue, L-phenylalanine-*p*-nitroanilide (Figure 7B). This analyte may not fit in the highest energy sites of the material and can thus only access less selective but more rapidly exchanging sites. This results in an efficient near baseline resolution of the racemate within a 3 min run time. Thus, the composite MIPs allow racemic resolutions with efficiencies in the order of commercial CSPs<sup>21</sup> as long as the sample load is high and/or only template analogue structures are injected. These commercial CSPs consist commonly of protein phases which in terms of the resulting elution profiles exhibit striking similarities with the imprinted phases.<sup>22</sup>

The number of theoretical plates ( $N$ ) for the D-enantiomer (the template antipode) on the thin film composites typically exceed  $2000 \text{ m}^{-1}$  (see, for instance, Figure 7A,  $C_R^{240}$ ), and at lower sample loads  $N$  may be considerably higher.<sup>11</sup> This indicates a much reduced hindrance to diffusion when

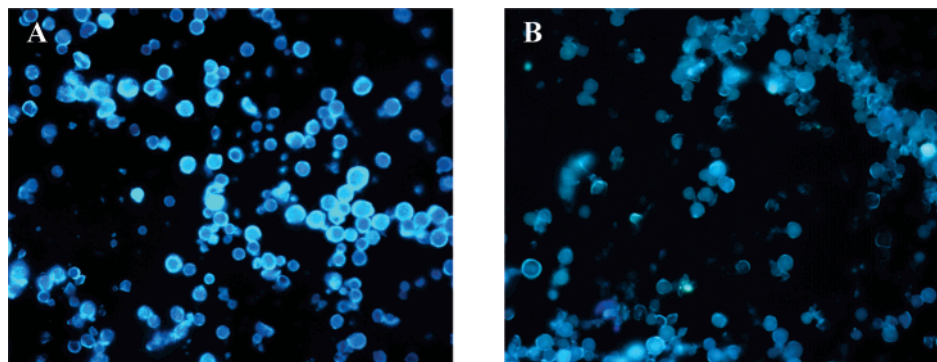


**Figure 5.** Fluorescence micrographs ( $40\times$  magnification) of (A) an imprinted composite ( $C_R^{60}$ ,  $d = 0.9$  nm) prepared in the presence of RAFT agent and (B) an imprinted composite ( $C^{60}$ ,  $d = 0.9$  nm) prepared without addition of RAFT agent. Thicknesses ( $d$ ) estimated based on %C.

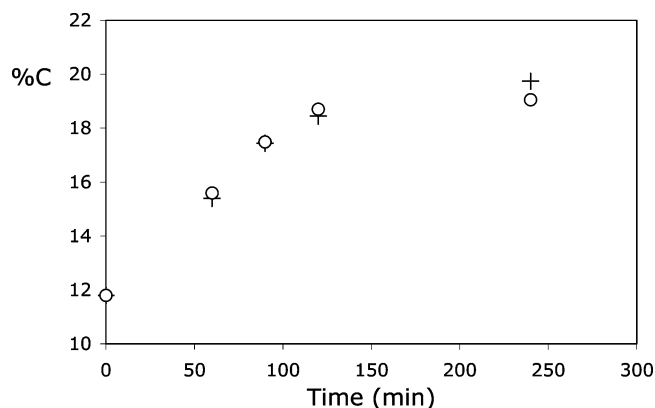


**Figure 6.** Carbon content of imprinted (crosses) and non-imprinted (circles) composites prepared as described in Table 2 by RAFT mediated grafting from Si-APS-ACPAB.

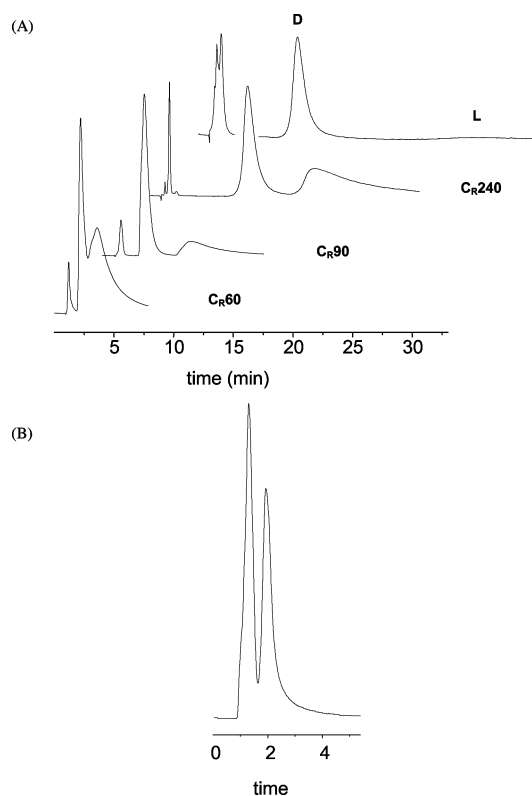


**Figure 7.** Elution profiles of (A) D,L-PA injected (10  $\mu$ L of a 1 mM solution) on columns (120  $\times$  4.5 mm) packed with the indicated L-PA imprinted composites prepared in the presence of RAFT agent and (B) D,L-phenylalanine-4-nitroanilide (10  $\mu$ L of a 1 mM solution) injected on  $C_R^{90}$ . The top profile in (A) was obtained by injecting a 0.5 mM solution of the racemate on  $C_R^{240}$ . Mobile phase: (A) MeCN/sodium acetate buffer, 0.01 M, pH 4.8, 70:30 (v/v), (B) MeCN/H<sub>2</sub>O/AcOH, 92.5:5:2.5 (v/v/v). The first eluting peak observed at low loads is due to breakthrough of both enantiomers. The number of theoretical plates for the nonretained void marker (acetone) was typically ca. 10 000/m.

compared to the conventional imprinted polymers which typically exhibit plate numbers around or below 1000  $m^{-1}$ .<sup>23</sup>

Although composites prepared under RAFT control do not lead to significant differences in the chromatographic behavior relative to materials prepared in the absence of RAFT control (see Supporting Information), the structure

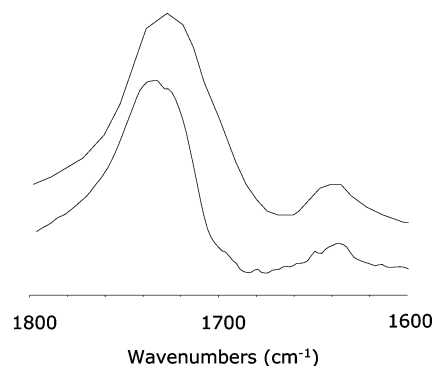


**Figure 8.** Expanded region of the FT-IR spectra of poly(MAA-co-EDMA) grafted under RAFT control to silica ( $C_R^{90}$ ; lower spectrum) and a corresponding solution polymerized sample prepared using soluble initiator in the absence of RAFT agent (upper spectrum).

of the grafted polymers and the mechanism of their formation should exhibit major differences. Upon the UV induced decomposition of the immobilized azo initiator the generated radicals may add monomer to propagate chains or be capped by RAFT agent. The relative rate constant for the exchange reaction  $C_{ex}$  ( $=k_{ex}/k_p$ , where  $k_{ex}$  is the rate constant for the exchange reaction (see eq 1) and  $k_p$  is the propagation rate constant) as defined by Fukuda et al. was estimated to be about 140 for the polymerization of methyl methacrylate using dithiobenzoates as RAFT agents.<sup>17</sup> Under typical conditions this implies that only a few monomers are inserted between each exchange reaction which promotes a degenerative chain growth. It has also been shown that an excess of initiating radicals leads to a quantitative incorporation of the RAFT agent in the polymer. Considering that each immobilized initiator molecule decomposes into one surface confined and one mobile radical and assuming an equal reactivity of the RAFT agent toward the resulting radicals or chains, the composites should contain about 370  $\mu$ mol/g of dithiobenzoate capping groups. In view of the sulfur microanalysis results (see Table 2), a maximum of 77  $\mu$ mol/g has been incorporated. This low incorporation agrees with the results reported by Baum and Brittain<sup>18</sup> and may be explained by the nature of surface termination reactions. As shown by Fukuda et al. the degenerative nature of the RAFT control allows radicals to essentially migrate in the surface layer leading to a higher probability of radical-radical recombination between two grafted chains.<sup>19</sup> This contrasts with the nature of the traditional “grafting from” process where termination via recombination between surface and solution propagating chains is much more common. This latter termination mechanism is less likely under RAFT control where the radical concentration is low.<sup>18</sup>

An important question refers to the extent and distribution of cross-links in the grafted films. Only few studies on the controlled radical polymerization (CRP) involving multifunctional monomers have appeared (for examples, see refs 14 and 24–27). One important reason is the loss of living

(24) Wang, A. R.; Zhu, S. *Macromolecules* **2002**, *35*, 9926–9933.

(25) Guan, Z. *J. Am. Chem. Soc.* **2002**, *124*, 5616–5617.

(26) Isaure, F.; Cormack, P. A. G.; Graham, S.; Sherrington, D. C.; Armes, S. P.; Bütün, V. *Chem. Commun.* **2004**, 1138–1139.

(27) Viklund, C.; Nordstrom, A.; Irgum, K.; Svec, F.; Frechet, J. M. J. *Macromolecules* **2001**, *34*, 4361–4369.

(21) Subramanian, G., Ed. *Chiral separation techniques*, 2nd ed.; Wiley-VCH: Weinheim, 2001.

(22) Mallik, R.; Jiang, T.; Hage, D. S. *Anal. Chem.* **2004**, *76*, 7013–7022.

(23) Sellergren, B.; Shea, K. J. *J. Chromatogr.* **1993**, *635*, 31–49.

properties and polymerization control that results from the diffusion controlled reactions occurring in polymerizations involving more viscous systems.<sup>24</sup> Copolymerization of methyl methacrylate and EDMA by ATRP showed a Tromsdorff effect, as in the absence of CRP and ESR radical signals that were identical to those observed in conventional radical polymerization of the same monomers.<sup>24</sup> On the other hand higher concentrations of chain transfer agents and low monomer concentrations allow EDMA to be solution polymerized resulting in hyperbranched architectures.<sup>25,26</sup> In our case the RAFT mediated polymerizations did not result in detectable physical differences. Comparing the FT-IR spectrum of a RAFT composite ( $C_R^{90}$ ) with that of a corresponding solution polymerized network revealed only small differences. Notably, the intensity of the band at  $1639\text{ cm}^{-1}$  assigned to the C=C stretch of pendent double bonds when normalized with reference to the C=O stretch at  $1730\text{ cm}^{-1}$  did not change (Figure 8).

This indicates that the materials exhibit a similar level of unreacted pendent double bonds which for the reference material is known to be in the order of 10%.<sup>23</sup> More striking is the lower surface areas measured for the RAFT composites. Interestingly, this was associated with a complete disappearance of the micropore surface which appeared in the native silica. Possibly the grafting leads to a more effective blocking of micropores or evening out of roughnesses as previously observed by Ruhe et al.<sup>28</sup>

## Conclusions

We have introduced a new approach to prepare thin films of imprinted polymers which combines covalent immobilization of azo initiators with RAFT-mediated living radical polymerization on preformed support material. The method should be adaptable to supports with different morphologies giving access to imprinted composites with different pore sizes, particle sizes, and morphologies exhibiting molecular recognition combined with superior mass transfer properties in relation to conventional solution polymerized networks.

**Acknowledgment.** We thank Zoefre Bayram-Hahn (Universitat Mainz) for assistance with the Nitrogen Adsorption Measurements, Monika Meuris (Universitat Dortmund) for the SEM micrographs, Fernando Tamayo (Universidad Europea de Madrid) for assistance in the synthesis of RAFT agent and initiator immobilization, and Dieter Lubda (Merk KGaA, Darmstadt, Germany) for the generous gift of silica materials. Financial support from DFG (Se777/5-2) is gratefully acknowledged.

**Supporting Information Available:** FT-IR transmission spectra, nitrogen adsorption/desorption isotherms, and elution profiles (PDF). This material is available free of charge via the Internet at <http://pubs.acs.org>.

CM052153X

---

(28) Ribbe, A.; Prucker, O.; Ruhe, J. *Polymer* **1996**, *37*, 1087–1093.